

# Influence of $^{60}\text{Co}$ $\gamma$ -Ray irradiation on the morphology of crystalline polyethylene studied by high-resolution solid-state $^{13}\text{C}$ NMR

ZHU QING-REN, HE PING-SHENG

*Structure Research Laboratory, University of Science and Technology of China, Hefei 230026, Anhui, People's Republic of China*

F. HORII, R. KITAMARU

*Institute for Chemical Research, Kyoto University, Uji, Kyoto 611, Japan*

The relationship and influence of varying  $^{60}\text{Co}$   $\gamma$ -ray irradiation doses, in the range 0.77–5.2 MGy, on the morphology of polyethylene have been investigated using high-resolution solid-state  $^{13}\text{C}$  nuclear magnetic resonance analyses through variation of different phase components,  $T_{1c}$ ,  $T_{2c}$  relaxation parameters, and line width. The cross-linking in the irradiated polyethylene takes place mainly in the non-crystalline regions. However, distortion and damage to the folded chain of the crystal lattice are observed in the crystalline regions. For the interfacial phase, both cross-linking and distortion could occur. As a result, part of the crystalline component transformed into a non-crystalline one. It was also found that the orthorhombic crystalline lattice transformed into a monoclinic one within the crystalline phase in polyethylene under higher doses of irradiation.

## 1. Introduction

Having applied cross-polarization (CP), magic-angle sample spinning (MAS) combined with dipolar decoupling (DD) to study the morphology and various kinds of molecular motion in different phases of crystalline polymers having less molecular motion, some mathematical methods have been created to obtain high-resolution solid-state nuclear magnetic resonance (NMR) spectra similar to that in a liquid [1–4]. Being different from solid broad-line NMR, the method is able to obtain information such as chemical shifts of every carbon in the molecular chain, relaxations  $T_1$ ,  $T_2$  and NOE, etc., and, therefore, to discuss the chemical structure of solid-state polymer, chain conformation and configuration, morphology and dynamic properties, in detail. Compared with X-ray diffraction studies, the method is also able to obtain information on structure in the non-crystalline region for a part-crystalline polymer.

To date, the mechanism of irradiation cross-linking and its influence on morphology and phase structure are not clear, although studies on irradiation effect of crystalline polyethylene have been under way for a long time. Some results obtained with several methods have been reported in recent literatures [5–7], but they are not consistent with each other. There is, to our knowledge, still no report concerning the problems relating to studies with high-resolution solid-state  $^{13}\text{C}$  NMR.

We have studied the phase structure of the crystalline polyethylene, analysed and characterized in detail

by means of high-resolution solid-state  $^{13}\text{C}$  NMR CP/MAS for polyethylene solid samples crystallized from the melt and dilute solution [3, 4], and reported that H-type cross-links and Y-type long branches were found to be significantly formed during the  $^{60}\text{Co}$   $\gamma$ -ray irradiation by solution-state  $^{13}\text{C}$  NMR spectroscopy [8, 9]. The work also showed the  $G$ -values of the H-links and Y-branches were 0.74 and 0.27, respectively, indicating that H-links are more effectively produced in the molten state than Y-branches for linear polyethylene.

The present paper reports our experimental results on the different phase structures obtained with high-resolution solid-state  $^{13}\text{C}$  NMR for polyethylene crystallized from a dilute solution, and blow-moulded film before  $^{60}\text{Co}$   $\gamma$ -ray irradiation above their gelation-forming doses. The relaxation behaviour of  $^{13}\text{C}$  NMR and change of phase component with increasing irradiation dose in crystalline, crystalline–amorphous interphase and rubber-like amorphous phases are also reported, and the effect of irradiation on crystalline polyethylene is discussed.

## 2. Experimental procedure

### 2.1. Samples

Sample I is a polyethylene with molecular weight (MW) of  $\bar{M}_n = 1.29 \times 10^4$ ,  $\bar{M}_w/\bar{M}_n = 1.5$  supplied by Showadenko Company, Japan. Having been prepared into a solution with concentration of 0.17 wt % in

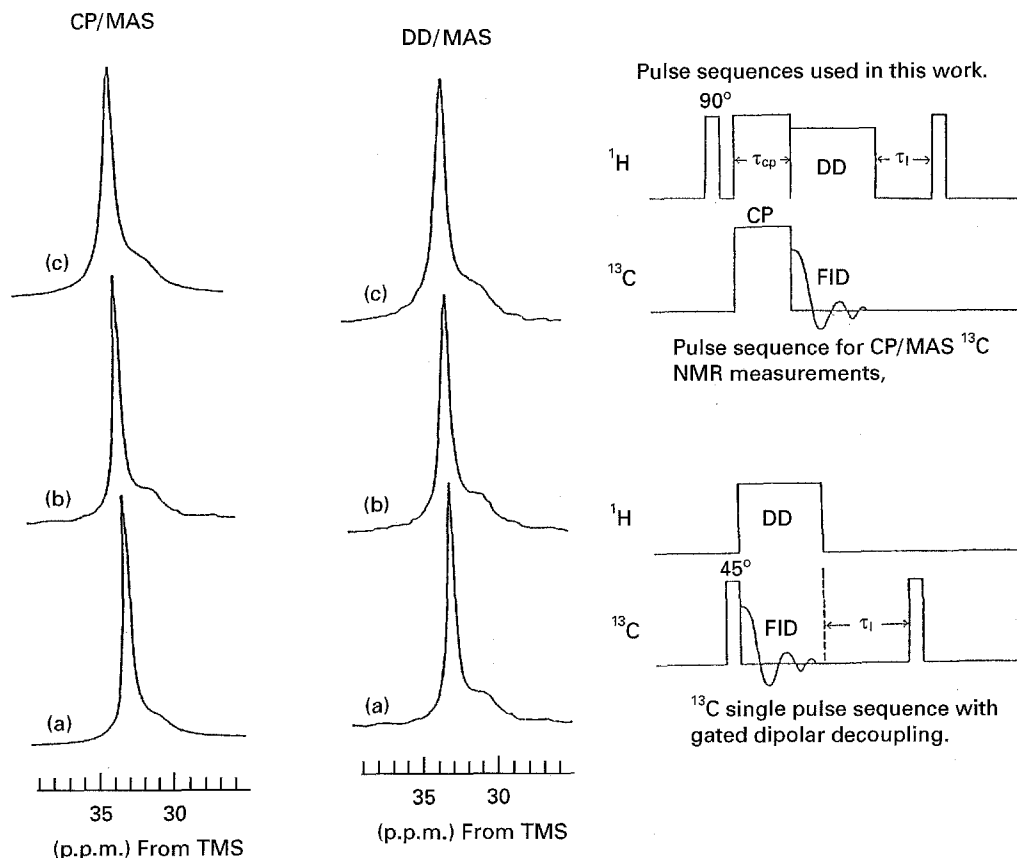


Figure 1 CP/MAS and DD/MAS  $^{13}\text{C}$  NMR spectra of unirradiated and irradiated films. (a) Unirradiated (F0), (b) irradiated (F200), (c) irradiated (F520).

xylene, the sample was crystallized isothermally in a bath of temperature  $85 \pm 0.1^\circ\text{C}$  in nitrogen for 30 h. The crystal powder was filtered and washed with acetone several times, then dried at  $50^\circ\text{C}$  in vacuum for 50 h. The sample prepared in this way is denoted SC0.

Sample II is a blow-moulded polyethylene film with molecular weight of  $\bar{M}_n = 0.84 \times 10^4$  made by the same Japanese company. After extraction by methanol, the sample film, denoted F0, was dried in a vacuum for 72 h, then cut into pieces of  $15\text{ mm} \times 4\text{ mm}$ .

## 2.2. $\gamma$ -ray irradiation

After degassing in a glass tube of 10 mm diameter in a vacuum of  $10^{-5}\text{ mm Hg}$  for 24 h, the samples were sealed in the tube. The irradiation rate of the cobalt source was  $17.4\text{ kGy h}^{-1}$ . The irradiation doses were 0.77 (SC75, F75), 2.39 (SC240, F240) and 5.20 (SC520, F520) MGy, respectively.

## 2.3. Measurement of high-resolution solid-state $^{13}\text{C}$ NMR

The measurements were carried out using a JNM-FX200 NMR apparatus with a solid magic rotating detector at room temperature. The field intensity,  $B_0$ , was 4.7 T, the resonant frequencies of  $^1\text{H}$  and  $^{13}\text{C}$  were 199.5 and 50.1 MHz, respectively, and the observed magnetic field strength,  $\gamma B_1/2\pi$  was 69.4 kHz ( $B_{1c} = 6.5\text{ mT}$ ,  $B_{1H} = 1.6\text{ mT}$ ). In order to avoid dis-

charge from the sample, the  $\gamma_H B_{1H}/2\pi = 54.3\text{ kHz}$  ( $B_{1H} = 1.3\text{ mT}$ ) during dipolar decoupling (DD), it is necessary to adjust  $B_{1H}$  and  $B_{1c}$  each time to meet the Hartmann-Hahn condition  $\gamma_H B_{1H} = \gamma_C B_{1c}$ . MAS experiments were carried out at a rate of 4.0–4.2 kHz with a cylinder-type rotator made of  $\text{Al}_2\text{O}_3$  and poly(amide-imide) resins, with a sample weight of about 0.1–0.2 g. The chemical shifts relative to tetramethylsilane were determined from the CH line (29.50 p.p.m.) of solid adamantane used as an external standard [10].

## 2.4. Computer analysis method

The data from the computer in the JNM-FX200 set were transformed into the IBM computer system in a standard form. The component separation of the spectrum and analysis of  $T_{1c}$ ,  $T_{2c}$  were performed on a FACOM 180 macrocomputer, assuming all spectra were Lorentzian. Having chosen suitable component spectra as a start value, the non-linear least squares method was performed to analog the data.

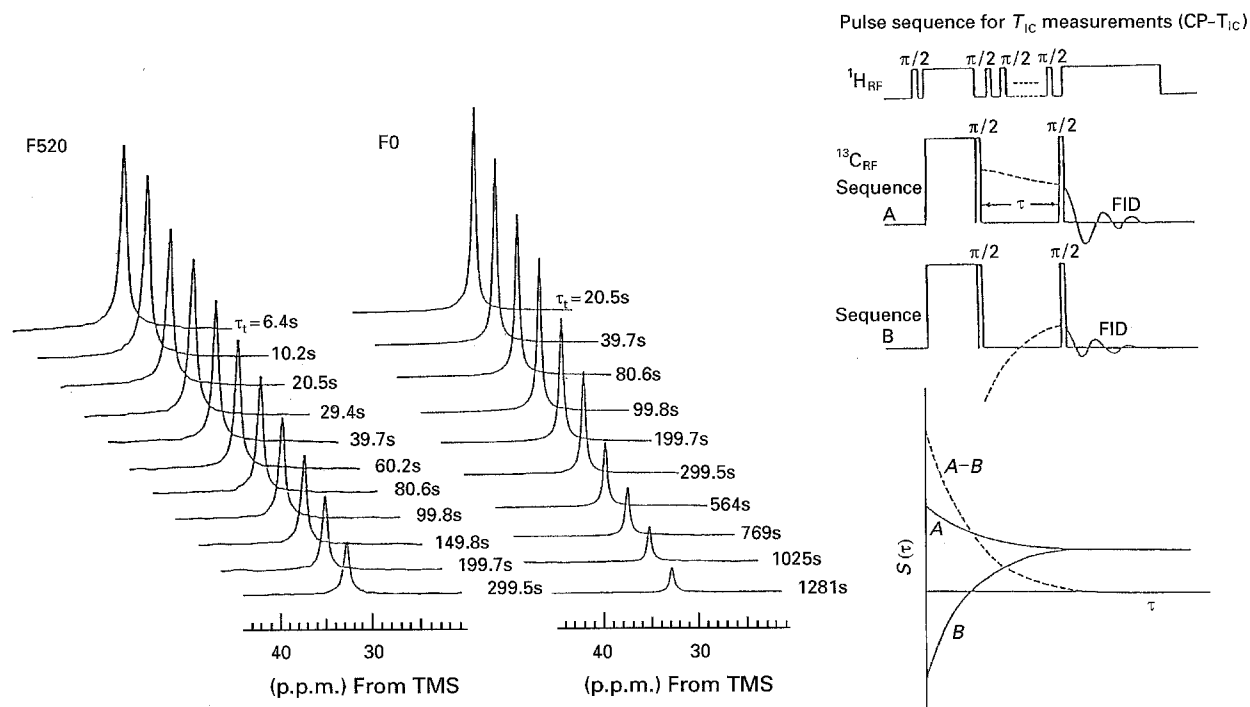
## 3. Results and discussion

### 3.1. High-resolution solid-state spectrum before and after irradiation

Fig. 1 shows CP/MAS and DD/MAS  $^{13}\text{C}$  spectra of blow-moulded film F0 at various doses of  $^{60}\text{Co}$   $\gamma$ -ray irradiation. The contact time was  $\tau_{cp} = 2\text{ ms}$  in CP

TABLE I  $^{13}\text{C}$  spin-lattice and spin-spin relaxation times of unirradiated and irradiated polyethylene samples

Sample	Irradiation dose (MGy)	$T_{1c}$ (s)				$T_{2c}$ (ms)	
		Crystalline		Noncrystalline		Interfacial	Rubbery
SC0	0	638	40.5	2.7	0.61	0.048	Unobserved
SC75	0.77	581	20.1	3.1	0.49	—	—
SC200	2.39	370	20.0	4.5	0.49	—	—
SC520	5.20	203	14.9	2.0	0.41	0.016	Unobserved
F0	0	655	77.9	2.5	0.56	0.054	1.10
F75	0.77	580	34.2	3.0	0.47	—	—
F200	2.39	477	31.3	4.8	0.46	0.041	0.68
F520	5.20	295	31.2	2.2	0.43	0.027	0.41


 Figure 2 Partially relaxed  $^{13}\text{C}$  spectra of unirradiated (F0) and irradiated (F520) films, measured by pulse sequence CP- $T_{1c}$ .

pulse, DD was a standard single pulse of  $45^\circ$ , and  $\tau_1$  was assumed to be three times the longest  $T_{1c}$  in the samples (also see Table I). Therefore, the DD/MAS spectrum responded to all the components in the spectrum. The chemical shift of peak A (33.0 p.p.m.) is the same as that of *n*-paraffin [10] and the average value,  $\sigma_{\text{ave}}$ , of the chemical shift was obtained from the  $\text{CH}_2$  chain with *trans-trans* isomer given elsewhere [3]. The chemical shift of peak B (31.0 p.p.m.) is in agreement with the  $\sigma_{\text{iso}}$  of the  $\text{CH}_2$  group in the polyethylene in molten state [11, 12]. Thus, peaks A and B should arise from the crystalline component in the orthorhombic crystalline system, and the rubber-like amorphous component, respectively, which can be confirmed by the experimental results of  $T_{1c}$  and  $T_{2c}$  in the next section.

In general, the CP effect of magnetic transformation from the  $^1\text{H}$  spin system to the  $^{13}\text{C}$  system under Hartman-Hahn conditions will increase with decreasing molecular motion of the chain for a multi-components system with various molecular motions in the solid. The facts that peak B in the CP/MAS spectrum

of sample F0 is weaker and the same peaks of F240 and F520 are stronger, reveal that some cross-linking structure has been formed in the amorphous region of the sample due to the irradiation, resulting in reduction of the molecular motion of the chain in the amorphous phase.

### 3.2. $^{13}\text{C}$ spin-lattice relaxation behaviour

Fig. 2 presents some  $T_{1c}$  relaxation spectrum of the long component in samples F0 and F520 measured by the CP- $T_{1c}$  method following the pulse sequence given by Torchia [13]. As can be seen in Fig. 2, it is possible to accumulate data by using the magnetic difference ( $A-B$ ) of  $A, B$  sequence and it is not necessary to wait for equilibrium of the vector of  $^{13}\text{C}$  NMR on the  $Z$ -axis [3], which will save much observation time for experiments with longer  $T_{1c}$ . If assuming a suitable  $\tau$  value, the component with shorter  $T_{1c}$  will disappear and it will only be possible to observe the component with longer  $T_{1c}$ . In our experiments, with  $\tau = 10$  s, the shoulder peak (peak B in the DD/MAS spectrum) of

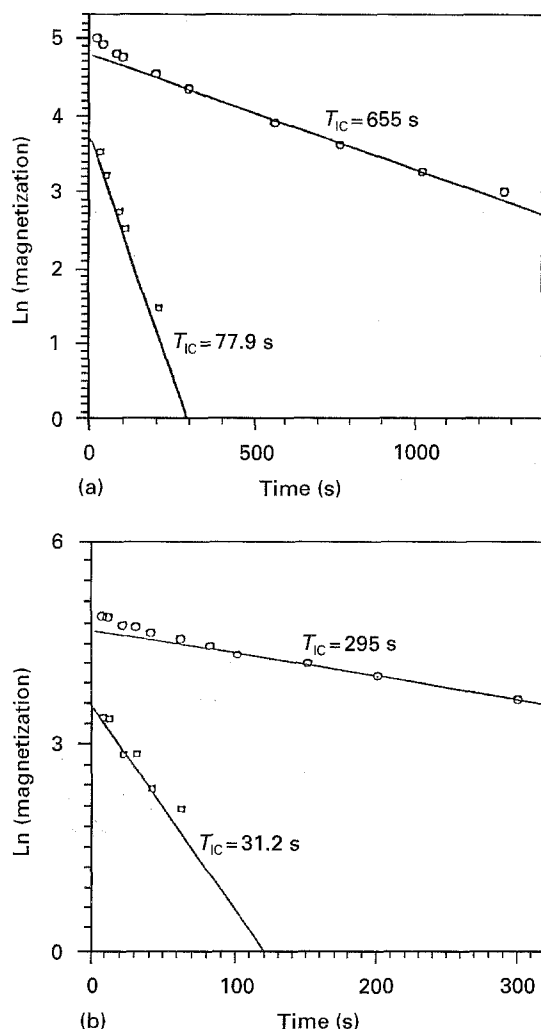


Figure 3  $^{13}\text{C}$  spin-lattice relaxation behaviour for samples (a) F0 and (b) F520.

high field in Fig. 2 disappears completely, from which the  $T_{1c}$  value of the amorphous component was estimated, and found to be less than several seconds.

Compared with the relaxation spectra of F0 and F520, the  $T_{1c}$  relaxation of the crystalline component becomes faster after irradiation. The relaxation curves of the longer component  $T_{1c}$ , obtained from different  $\tau_t$  and intensities by using figure analysis of the non-linear least mean method on computer, are shown in Fig. 3. Obviously it is not possible to describe the delay curve of magnetic intensity with a single exponent form. However, it consists of two parts, A and B, with a turning point

$$M = 2M_{cp}^A \exp(-\tau/T_{1c}^A) + 2M_{cp}^B \exp(-\tau/T_{1c}^B) \quad (1)$$

Based on this formula, the results calculated by computer indicate that there are two different  $T_{1c}$  values, i.e.  $T_{1c}^A$  and  $T_{1c}^B$  (Fig. 3).

The SR method was applied for measurement of the component with shorter  $T_{1c}$ . Fig. 4 is the relaxation spectrum of  $T_{1c} < 10$  s measured using the SR method. Besides the amorphous component of high field (B peak), it also includes the relaxation with shorter  $T_{1c}$  component in the low-field crystalline

component (peak A). Fig. 5 shows the intensity of the low-field crystalline peak A after computer treatment; the solid line is the theoretical curve calculated based on assuming two existing  $T_{1c}$  values of 2.5 and 77.9 s for F0, and 2.2 and 31.2 s for F520, respectively. The longer value is almost the same as the shorter value of the two  $T_{1c}$  (B) determined with the CP- $T_{1c}$  method. On combining the experimental results obtained from the two types of pulse, it can be concluded that three kinds of component exist with  $T_{1c}$  values of several hundreds, several decades and several seconds, respectively.

The same method has been applied to observe  $T_{1c}$  for the amorphous component at  $\gamma = 31.0$  p.p.m. (peak B) and found that there is only a single value of more than 0.4–0.5 s.

The  $T_{1c}$  values before and after irradiation are listed in Table I. The factor determining the  $T_{1c}$  value is the fast motion of local chain sequence with a high frequency of  $10^8$  Hz; therefore, it is not difficult to understand that there are three types of short-range motion mode in the crystalline phase and only one type in the amorphous phase [4]. Both the largest  $T_{1c}$  in the crystalline phase of the two samples obviously decrease with increasing  $\gamma$ -ray irradiation. After irradiation,  $T_{1c}$  was reduced to half its original value, but virtually no change was observed for the two shorter  $T_{1c}$ . The crystalline component with larger  $T_{1c}$  is the main part of the whole crystalline phase, and it is considered to be the main stiff component with typical lamellar thickness. In addition, the molecular chain motion in the crystalline component responding to  $T_{1c}$  also includes the diffusion from the crystalline phase to the amorphous one; thus the fact that  $T_{1c}$  decreases above 0.77 MGy doses of irradiation indicates that some decomposition or failure has occurred in the crystalline region, a result of the decrease of lamellar thickness.

In addition,  $T_{1c}$  values in the amorphous component decrease with increasing irradiation doses for both samples, indicating that cross-linking between molecular chains has been formed due to irradiation; therefore, some molecular motions are forbidden and  $T_{1c}$  decreases.

### 3.3. $^{13}\text{C}$ spin-spin relaxation

Fig. 6 represents the experimental  $T_{2c}$  relaxation spectra. There is a very short  $T_{1c}$  in the low-field crystalline peak when  $\tau_t = 3$  s. Peak B is still observed in sample F0 even when  $\tau_t = 1000$   $\mu\text{s}$ , indicating that there is a rubber-like amorphous component with higher mobility in the sample. Two components corresponding to fast decline and slower decline, respectively, in the range of 200  $\mu\text{s}$  could be obtained from a plot of peak intensity against  $\tau_t$ , and  $T_{2c}$  could be found, using the same analysis method as before, to be 0.054 and 1.10 ms. The shorter  $T_{2c}$  should belong to the interphase component where the molecular chain is more or less limited [3, 4], and the longer  $T_{2c}$  spin-spin relaxation is related to a rubber-like amorphous component with larger molecular mobility.  $T_{2c}$  describing the slower long-range mobility of the

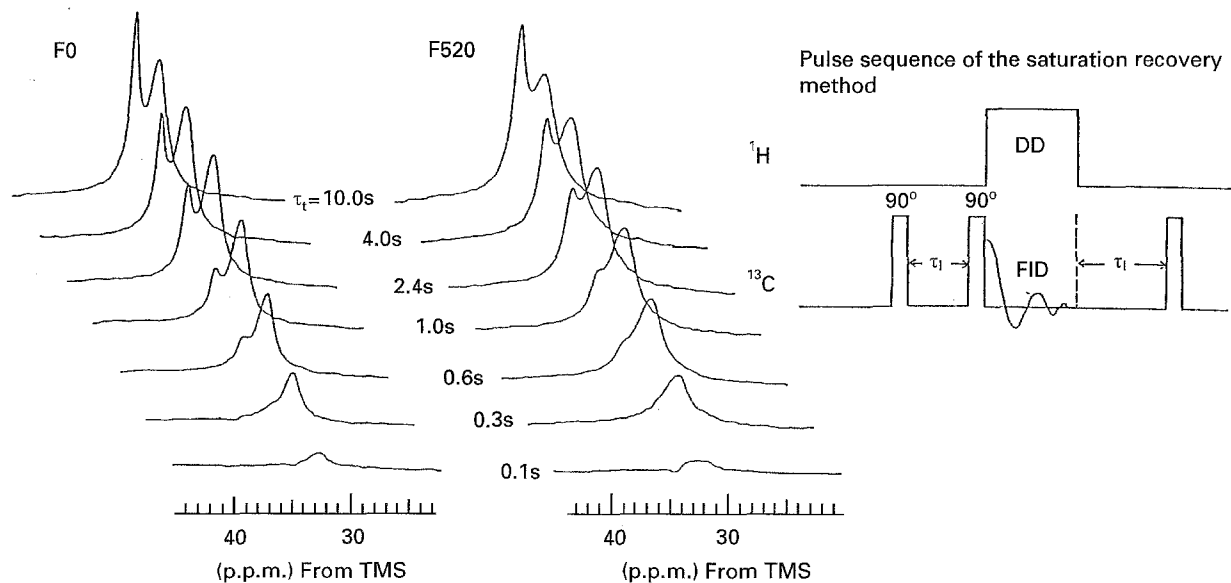


Figure 4 Partially relaxed  $^{13}\text{C}$  spectra of unirradiated (F0) and irradiated (F520) films, measured by the saturation method.

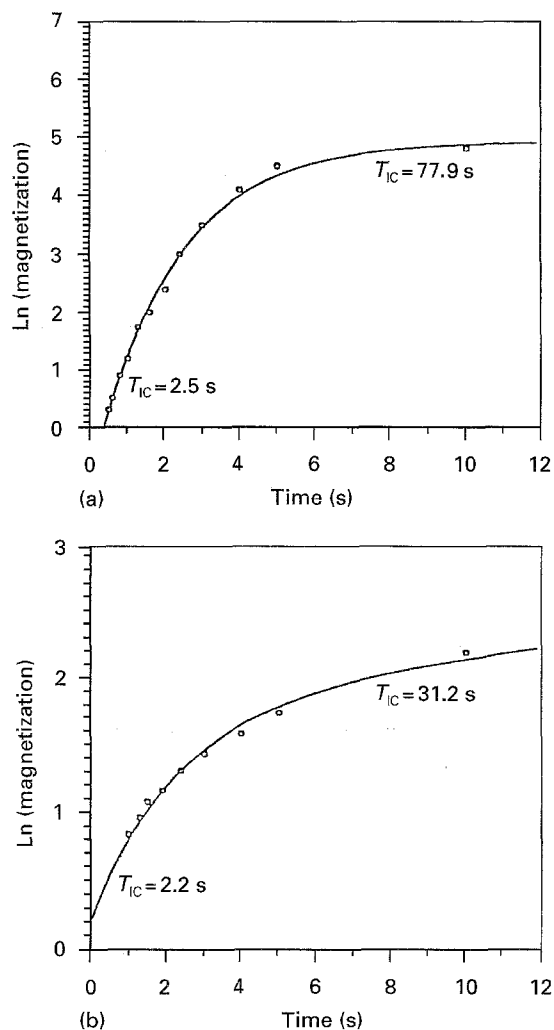


Figure 5  $^{13}\text{C}$  spin-lattice relaxation behaviour measured for samples (a) F0 and (b) F520 by the saturation recovery method.

molecular chain around zero frequency. There are two  $T_{2c}$  values in the amorphous region, where there was only one  $T_{1c}$  as before, corresponding to two types of long-range motion in the interphase and rubber-like amorphous phase.

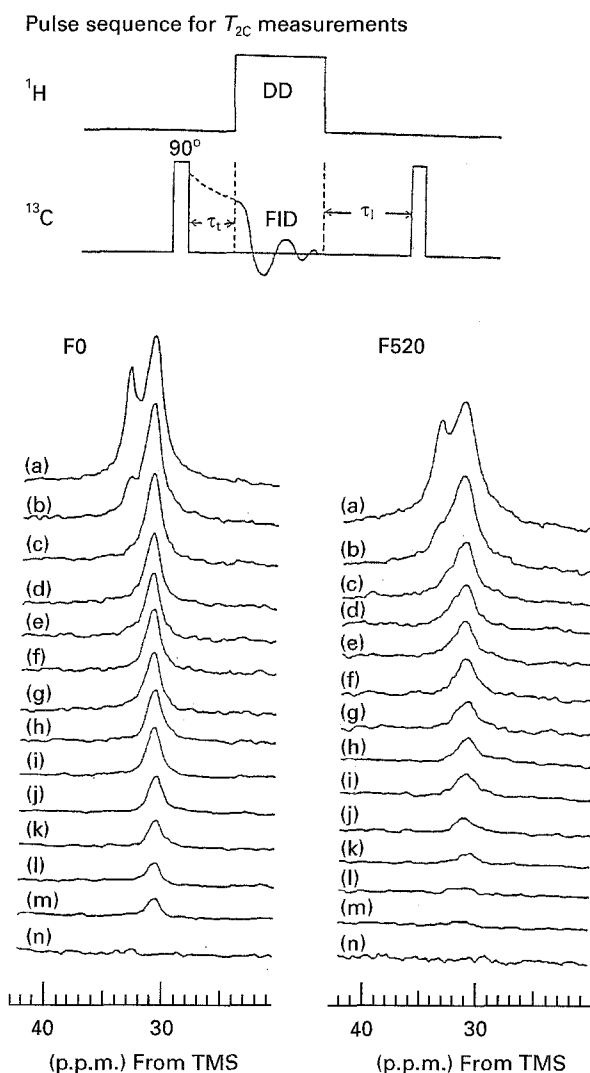


Figure 6 Partially relaxed  $^{13}\text{C}$  spectra of F0 and F520, measured by  $T_{2c}$  pulse sequence with  $\tau_1 = 3$  s.  $\tau_1$  ( $\mu\text{s}$ ): (a) 0.5, (b) 20, (c) 40, (d) 60, (e) 80, (f) 100, (g) 140, (h) 180, (i) 250, (j) 400, (k) 600, (l) 800, (m) 1000, (n)  $3 \times 10^5$ .

It has been confirmed that no rubber-like amorphous phase exists in sample SC0 crystallized from solution [3, 4]; therefore, only one  $T_{2c}$  of the

TABLE II Linewidths and mass fractions of the respective components of unirradiated and irradiated polyethylene samples

Sample	Irradiation dose (MGy)	Linewidth (Hz)				Mass fraction			
		C <sub>1</sub> <sup>a</sup>	C <sub>2</sub> <sup>b</sup>	I <sup>c</sup>	R <sup>d</sup>	C <sub>1</sub> <sup>a</sup>	C <sub>2</sub> <sup>b</sup>	I <sup>c</sup>	R <sup>d</sup>
SC0	0	32.7	112.0	104.7	Unobserved	79.6	6.4	13.9	0
SC75	0.77	32.9	128.1	113.6	Unobserved	75.7	9.1	15.2	0
SC200	2.39	35.3	134.2	116.6	Unobserved	71.5	8.2	20.4	0
SC520	5.20	45.9	140.6	175.7	Unobserved	59.8	18.0	22.2	0
F0	0	29.5	37.5	121.3	61.0	71.4	4.2	13.5	10.9
F75	0.77	30.1	61.5	126.6	72.2	67.9	5.7	13.9	12.5
F200	2.39	36.3	83.7	139.0	79.0	65.4	5.9	14.1	14.6
F520	5.20	47.5	137.0	206.0	117.0	59.6	6.7	14.5	19.2

<sup>a</sup>) Orthorhombic crystalline component.

<sup>b</sup>) Monoclinic crystalline component.

<sup>c</sup>) Interfacial component.

<sup>d</sup>) Rubbery component.

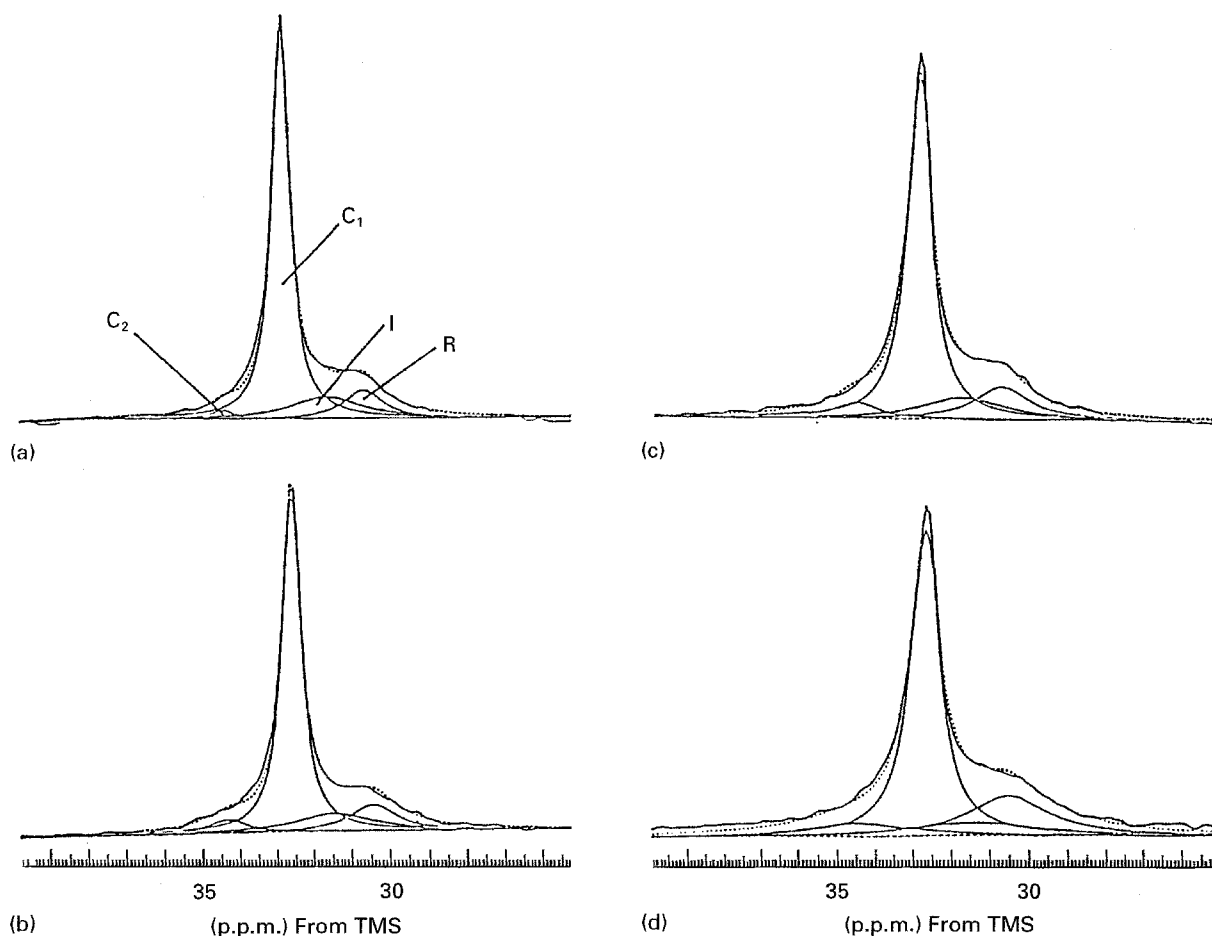


Figure 7 Component analysis of DD/MAS <sup>13</sup>C NMR spectra of polyethylene films and their irradiated samples. C<sub>1</sub>, orthorhombic crystalline component; C<sub>2</sub>, monoclinic crystalline component; I, interfacial component; R, rubbery component. (a) F0, (b) F75, (c) F200 and (d) F520.

interphase in the amorphous region could be observed (Table I).  $T_{2c}$  values of the other sample are also listed in Table I.

$T_{2c}$  values of the amorphous region (interphase and rubber-like components) in both samples decrease with increasing irradiation intensity, revealing that some cross-linking has been formed there, which is in agreement with the experimental results of  $T_{1c}$ . The formation of a three-dimensional cross-network limits long-range molecular motion, resulting in a decrease of  $T_{2c}$ .

### 3.4. Separation and analysis of multi-components of the spectrum

It is possible quantitatively to separate the contributions of different components from the whole DD/MAS spectrum knowing the shapes of every component spectrum. It is assumed that the spectrum containing only the rubber-like phase with  $\tau_1 > 80 \mu s$  (Fig. 6e-n) is approximately Lorentzian, and although there are three types of  $T_{1c}$  values in the crystalline peak, it is also possible to assume that they include a Lorentzian shape. Therefore, having used the

difference between spectrum a ( $\tau_1 = 0.5 \mu\text{s}$ ) and spectrum f ( $\tau_1 = 100 \mu\text{s}$  and linewidth = 61 Hz) in Fig. 6, the interphase component spectrum can be obtained and its chemical shift is 31.3 p.p.m., linewidth 121 Hz. Based on the data obtained, the DD/MAS spectrum for every sample could be analysed by the non-linear least squares method with a computer. The resulting mass fractions of crystalline, interphase and rubber-like components are listed in Table II.

It is necessary to introduce a fourth component peak, i.e. the crystalline component of the monoclinic crystal system [14] in order for it to be completely coincident with that of the spectrum observed experimentally (Fig. 7). The difference between the chemical shift in the monoclinic system and that in the orthorhombic crystal system should be attributed to different states of chain stacking.

The data in Table II show that the components of the orthorhombic crystalline system in both samples decrease with increasing irradiation intensity, that is they agree with the conclusion of thinning lamellae as well as decrease of the longer  $T_{1c}$ . Therefore, rubber-like phase and interphase components increase. The main change is the increase of the rubber-like phase in sample F0, but the interphase component from orthorhombic system in sample SC0, which does not originally have a rubber-like component, has an increasing rubber-like component due to irradiation. Under 5.2 MGy irradiation doses, a considerable amount (about three times) of the orthorhombic crystalline system changes into the monoclinic one, being a type of crystalline transition. In addition, the spectrum lines of components in the interphase and crystalline phase obviously widen with increasing irradiation, indicating a regular arrangement of chains in the crystalline phase, and *trans-trans* conformation of chains in the interphase with some regularity becoming disordered, resulting in a wide contribution to the conformation.

#### 4. Conclusions

After 0.77–5.20 MGy  $^{60}\text{C}$   $\gamma$ -ray irradiation, the change in morphology,  $^{13}\text{C}$  nucleus relaxation and mass distribution in various phases observed with  $^{13}\text{C}$  high-resolution solid-state NMR of polyethylene can be summarized as follows.

1. The cross-linking by  $\gamma$ -ray irradiation occurred in the amorphous phase and interphase with higher mobility, that it agreed with the results obtained by Keller [6]. At the same time, the folded-chain structure is deformed, and even failed in the crystalline phase due to irradiation, resulting in thinning of lamellar thickness and reduction of its size.

2. The crystalline phase transforms into the interphase due to irradiation in sample SC0 with a higher crystalline degree and no rubber-like phase. If the irradiation intensity is quite high, the crystalline type changes within the crystal would mainly occur, i.e. change from an orthorhombic crystal system into a monoclinic one. For sample F0, with lower crystalline degree and rubber-like phase, transformation of phases obviously exists, i.e. transformation from orthorhombic into amorphous.

#### References

1. J. SCHAEFER and E. O. STEJSHAL, *J. Am. Chem. Soc.* **98** (1976) 103.
2. C. H. YE, *Chinese J. Magn. Res.* **1** (1984) 415.
3. R. KITAMARU, F. HORRI, Q. R. ZHU, D. C. BASSETT and R. H. OLLEY, *Polymer* **35** (1994) 1171.
4. R. KITAMARU, F. HORRI and K. MURAYAMA, *Macromolecules* **19** (1986) 636.
5. M. DOLE and N. GVOZDIC, *J. Polym. Sci. Polym. Phys. Ed.* **18** (1980) 169.
6. A. KELLER and G. UNGAR, *Rad. Phys. Chem.* **22** (1983) 155.
7. G. Y. HUANG, N. Y. CHEN and B. Z. JIANG, *Appl. Chem.* **4** (1987) 26.
8. F. HORRI, Q. R. ZHU, R. KITAMARU and H. YAMAOKA, *Macromolecules* **23** (1990) 977.
9. Q. R. ZHU, F. HORRI, R. KITAMARU and H. YAMAOKA, *J. Polym. Sci. Part A Polym. Chem.* **28** (1990) 2741.
10. W. L. EARL and D. L. VANDERHART, *J. Magn. Res.* **48** (1982) 35.
11. T. HAMA, T. SUZUKI and K. KOSAKA, *Kobunshi Ronbunshu* **32** (1975) 91.
12. F. HORRI, K. MURAYAMA, M. NAKAGAWA, Q. R. ZHU and R. KITAMARU, *Polymer Preprints Jpn* **34** (1985) 340.
13. D. A. TORCHIA, *J. Magn. Res.* **30** (1978) 613.
14. D. L. VANDERHART and F. KHOURY, *Polymer* **25** (1984) 1589.

Received 9 August  
and accepted 21 December 1995